DOI: 10.32615/ps.2020.004 PHOTOSYNTHETICA 58 (SI): 422-432, 2020

Special issue in honour of Prof. Reto J. Strasser

Influence of *Cuscuta campestris* Yunck. on the photosynthetic activity of *Ipomoea tricolor* Cav. – *in vivo* chlorophyll *a* fluorescence assessment

L. ZAGORCHEV[*,**,+], A. TRAIANOVA[**], D. TEOFANOVA[**], J. LI[*], M. KOUZMANOVA[**,+], and V. GOLTSEV[**]

Zhejiang Provincial Key Laboratory of Plant Evolutionary Ecology and Conservation, Taizhou University, 318000 Taizhou, China[*]
Faculty of Biology, Sofia University 'St. Kliment Ohridski', 8 Dragan Tsankov Blvd, 1164 Sofia, Bulgaria[**]

Abstract

Cuscuta campestris Yunck. is a parasitic plant, acquiring nutrients from the hosts. Although a generalist, its hosts differ in their susceptibility. *Ipomoea tricolor* Cav. is a semi-compatible host – *C. campestris* growth is restricted in infected plants. We aimed to assess the effect of the parasite on this semi-compatible host by using the sensitive JIP-test to follow physiological changes in leaves at different vegetative stages – aged, mature, and newly emerging. The characteristics of the photosynthetic machinery were estimated by 17 parameters, calculated from the prompt chlorophyll *a* fluorescence. The most sensitive were performance index of photosystem II, performance index of photosystems I + II, and number of Q_A redox turnovers until maximal fluorescence is reached. The infected *I. tricolor* plants responded to the parasite by activating the electron transport in PSII in later periods. The oldest leaves and the youngest leaves developed certain adaptation to the parasite but the younger did not. The effect of the parasite on the photosynthetic apparatus depended on the physiological age of the host plant leaves.

Additional key words: haustoria; holoparasitic plant; photosystem I; photosystem II; stem parasite.

Introduction

Originally a North American species, the field dodder, *Cuscuta campestris* Yunck., have been introduced and spread worldwide, causing significant ecological and agricultural problems (Parker 2012). *Cuscuta campestris* is a stem holoparasitic plant. It penetrates the stem or leaves and establishes connection to the xylem and phloem of the host plants, extracting water and nutrients. The organ of parasitism – haustoria, is common for all parasitic plants, although anatomical and physiological differences exist between different families (Yoshida *et al.* 2016).

C. campestris is considered a nonphotosynthetic heterotrophic plant, although it retained most of the photosynthesis-related genes and chloroplasts, and has limited photosynthetic ability under certain conditions (Revill *et al.* 2005, McNeal *et al.* 2007). Carbon dioxide fixation in *Cuscuta* does not produce the final metabolites (sugars and phosphorous esters) of the Calvin cycle but metabolites (such as pyruvate, malate, and aspartate) which are involved in CO_2 uptake and storage (Dinelli *et al.* 1993).

Competition for water and solutes is unlikely to play a major role in determining decrease in host productivity: metabolic incompatibility is suggested to be the major cause (Press *et al.* 1990). Significant amount of the assimilated carbon could be transferred continuously from the host to the parasite, thus depleting the host resources and restricting its growth and development (Jeschke and Hilpert 1997). Increase in photosynthetic rates, in order to compensate for this carbon flow, was proposed and shown in certain cases (Jeschke *et al.* 1997, Jeschke and Hilpert 1997). In many other studies, however, the parasite was shown to restrict host's photosynthesis, *e.g.*, *C. campestris* and the closely related *C. australis* R. Br. parasitism on *Mikania micrantha* Kunth (Shen *et al.* 2007, Yu *et al.* 2011, Le *et al.* 2015) and *C. campestris* infested *Beta vulgaris* L. and *Medicago sativa* L. (Sarić-Krsmanović *et al.* 2018). Such reports suggest that dodders' influence on the host metabolism is not restricted to nutrients exhaustion and

Received 1 September 2019, *accepted* 8 January 2020.
[+]Corresponding author; e-mail: lzagorchev@biofac.uni-sofia.bg, kouzmanova@uni-sofia.bg
Abbreviations: Chl – chlorophyll; DC – differential curves; IC – induction curves; N – number of Q_A redox turnovers until maximal fluorescence is reached; OEC – oxygen-evolving complex; PF – prompt chlorophyll *a* fluorescence; PI_{ABS} – performance index of photosystem II; PI_{total} – performance index of photosystems I + II; PQ – plastoquinone; PSA – photosynthetic apparatus; RC – reaction center.
Acknowledgements: This work was supported by the Talented Young Scientist Program of the Ministry of Science and Technology of People's Republic of China.

some other mechanisms exist.

Impact of *Cuscuta* species, especially *C. reflexa* and *C. campestris*, on host biomass, photosynthesis, and source-sink relations has been studied extensively. It was found that *C. campestris* infection prevented flowering of *M. micrantha* and caused almost complete death of the aerial parts of the host in about 70 d (Shen *et al.* 2005, 2007). *Cuscuta campestris* infection significantly reduced the light-utilization efficiency and light-saturation point of the host, which led to reduced net photosynthetic rate of the fully expanded mature leaves. Besides resource capture by *C. campestris*, the decreased photosynthesis resulted in reduced growth of the infected *M. micrantha* plants – reduced total biomass, changed biomass allocation patterns, a reduced number of leaves, leaf area, stem length, and biomass. Total biomass of the infected host and the parasite was significantly lesser than that of the uninfected plants (Shen *et al.* 2005, 2007). Severe inhibition of growth and dry matter accumulation in the host plants was found in the presence of *C. reflexa*, but the total biomass of host plus parasite was almost the same as that of uninfected plants (Jeschke *et al.* 1997, Jeschke and Hilpert 1997, Press *et al.* 1999). This is a result of activated photosynthesis in host plants as a reaction to compensate the powerful sink of the parasite. It seems that there is not a common mode of how a parasite affects host photosynthesis.

Although *C. campestris* is considered a generalist, *e.g.*, feeding on multiple host species, which determines its wide success, and hosts may differ in their susceptibility to infection. Tomato (*Lycopersicon esculentum* Mill.), belonging to the same order as dodder – Solanales, family Solanaceae, and *Ipomoea* spp., belonging to the dodder's family (Solanales, Convolvulaceae) are known as fully or partially tolerant (Singh and Singh 1997). Assuming that dodder's effect on host's photosynthesis is not simply a resource-depletion event, a question has risen whether such effect would be also exhibited in a semi-compatible host-parasite interactions.

Illumination of dark-adapted leaf tissue leads to prompt chlorophyll (Chl) *a* fluorescence (PF), and the obtained curves provide information about functioning and structure of the photosynthetic apparatus (Kautsky and Hirsch 1931, Strasser *et al.* 2000). The PF induction curves (IC) were named O-J-I-P. The approach based on analysis of transient Chl *a* fluorescence is known as JIP-test (Strasser *et al.* 2004). The characteristic name, JIP-test, originates from the specific points on the curves of PF signal (Tsimilli-Michael and Strasser 2013a). Chl *a* fluorescence IC are based on the theory for energy flux in thylakoid membranes (Strasser *et al.* 2000). PF measurements provide information about plants physiological condition, especially about PSII and electron transport chain in light-dependent phase of photosynthesis (Tsimilli-Michael and Strasser 2008, 2013b). PSII in thylakoid membranes is the first component in plants, which can react to even the smallest distortions in plant functioning (Stirbet and Govindjee 2011). Measuring the Chl *a* fluorescence *in vivo* is a cheap, easy, noninvasive, informative, and highly sensitive method to observe the first symptoms of stress in plant organisms (Tsimilli-Michael and Strasser 2008). The JIP-test has become one of the popular tools in photosynthetic investigations (Strasser *et al.* 2010, Chen *et al.* 2014, Kalaji *et al.* 2014a,b; Zhang and Liu 2016).

The review of the available literature showed that effects of the parasite on the host are different, and can be expressed in suppression or activation of biomass production, which is also associated with modification of photosynthetic activity in the host leaves. *In vivo* measurements of Chl *a* fluorescence are a suitable approach to follow changes in the light reactions of photosynthesis in infected semi-compatible host plant because of the JIP-test high sensitivity. Analysis of OJIP kinetics can be useful tool for assessment of the environment impact on photosynthetic organisms, including effects of parasitic plants on host. The aim of this study was to investigate effects of parasite plant *Cuscuta campestris* on PF in leaves of different ages of the semi-compatible host plant *Ipomoea tricolor*.

Materials and methods

Growing of *Ipomoea tricolor* plants: *Ipomoea tricolor* Cav. certified seeds were purchased from a local supplier – *Sortovi Semena PLC*, Sofia, Bulgaria. Seeds were directly germinated in commercial peat substrate/perlite mixture. Plants were grown in growth chamber under 16/8-h (light/dark) photoperiod at 25°C. Light was provided by a *Kingbo KB-GLX45* full spectrum LED light, 140 μmol(photon) m^{-2} s^{-1}. The peat substrate for leafy ornamental plants by soil producer *JSC 'Durpeta*', Lithuania, was used (distributor – *G.B.M. Commerce Ltd.*). The peat substrate complies with the European requirements and Bulgarian State Standard no. 12580.

Cuscuta campestris seeds were from the laboratory collection of Sofia University – Telish population, Cherven Briag municipality, Pleven province, the Danubian plain, Bulgaria (GPS 43°19'27.3"N, 24°15'15.8"E), voucher herbarium SO 107784 in the Herbarium SO (Sofia University 'St. Kliment Ohridski'). Seed were surface-sterilized and seed coat was removed by 15 min incubation in concentrated H_2SO_4, then placed on water-soaked filter paper in a Petri dish and germinated at 30°C, for 48 h.

Infection of *I. tricolor* plants with *C. campestris*: The experiment was conducted in November–December with ten pots with *I. tricolor*, five of which were infected with *C. campestris*. The infection was done at the stage of fully developed second non-embryogenic leaf (28–30 d of vegetation), when the plants were briefly moved to a glasshouse under natural sunlight for approximately three days. *C. campestris* seedlings of 2–3 cm length were placed close to host plants and the host-parasite pairs were moved back to the growth chamber when macroscopically visible haustoria were formed.

Chl *a* fluorescence measurements: The prompt Chl *a* fluorescence was measured using *MPEA* fluorometer (*Hansatech Instruments Ltd.*, Norfolk, UK) after a dark adaptation for about 60 min, at the middle part of the leaf

blade. The PF protocol included 1-s pulse with high light intensity of 4,000 μmol(photon) m^{-2} s^{-1}.

The Chl *a* fluorescence measurements started when the first non-embryonic leaves (marked as L1 on Fig. 1*A*) had grown enough to be measured – after 15 d of vegetation, 0 d of the measurements. They were the oldest leaves, and their Chl fluorescence was measured during the entire experimental time, *i.e.*, 0–35 d (Fig. 1*B*). After 28 d, most of L1 were withered, and just few were measured. The measurements of the younger, second true leaves – L2, started 4 d later (19 d of vegetation), and they partially aged during the experiment. For the third, youngest leaves – L3, the first measurement was carried out 18 d after the beginning of the experiment (33 d of vegetation). Control plants were measured simultaneously at the same age leaves and at the same days.

JIP-test parameters used for evaluation of effects of parasite *C. campestris* on structure and functioning of *I. tricolor* were calculated from the obtained data for Chl *a* fluorescence on the base on the equations given by Strasser *et al.* (2004) and Stirbet and Govinjee (2011). They are presented in Appendix.

Statistical analysis: The experiment was carried out with ten equally developed plants, randomly divided into control group and *C. campestris*-infected group. Some of the leaves became yellowish and died during the senescence, so the Chl fluorescence cannot be measured. That is why the number of the samples had been reducing during the experiment. Average values of the induction curves and standard errors were calculated for all the investigated groups and times as follow: for control L1 from 16 to 6 measurements for each curve from 0 to 25 d, average of three measurements for 28, 30, and 32 d, and one measurement only for 35 d (most of the leaves were already withered); for control L2 leaves – between 12 and 6 measurements; for control L3 leaves – 6 measurements for all the investigated times; for the three groups of leaves of different age – L1, L2, and L3, from infected plants 5 measurements were averaged, with exception L1 on 35 d – 4 measurements (one leaf had withered); and L3 on 18 d – 2 measurements (L3 leaves in the other three pots were still not developed).

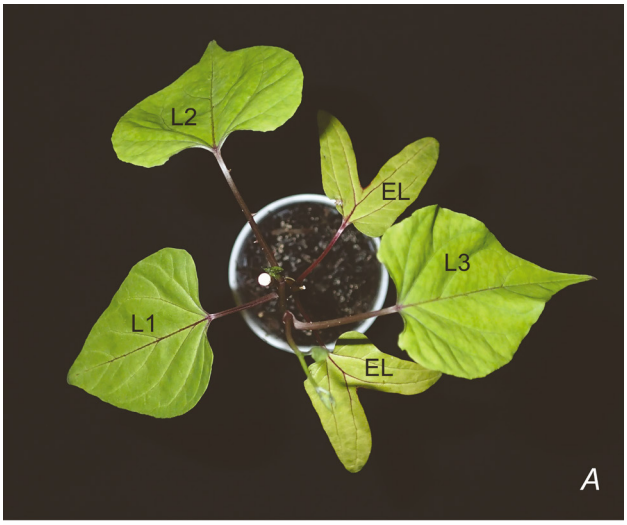

Vegetation days	15	19	28	29	30	31	33	36	40	43	47	50
Infection, days of the experiment			13	14	15							
Measurements/ day of the experiment												
L1	0					16	18	21	25	28	32	35
L2		4	*Infection*			16	18	21	25	28	32	35
L3							18	21	25	28	32	35

B

Fig. 1. Experimental design. (*A*) System of numbering of *Ipomoea tricolor* leaves. (*B*) Schematic of the time period of measurements, showing the actual vegetation days to which the measurement days correspond. EL – embryonic leaf; L1, L2, and L3 – leaves 1, 2, and 3, respectively.

Results and discussion

***Cuscuta campestris* infection and growth**: The initial stages of *C. campestris* parasitism on *I. tricolor* were relatively fast. Coiling was observed within 24 h, and haustoria were formed within 48–72 h of *C. campestris* seedlings placement in the pots with *I. tricolor*. Successful penetration and establishment of connection with the vascular elements of the host was confirmed microscopically (Fig. 2*A–C*). The further development of the parasite was highly restricted (Fig. 2*D*). Approximately 30% of the *C. campestris* plants did not developed at all. The growth rate of the others was very slow and by the end of the experiment the stem length ranged between 2 and 6 cm.

After 35 d of the experiment, the first true leaves (L1) in the control *I. tricolor* plants were significantly changed to completely yellow, while the remaining two types of leaves (L2 and L3) retained their green color and functional activity (Fig. 3*A*). In infected with *C. campestris* plants, L1 were still green after 35 d, but the color of younger L1 and L3 was more pale compared to control leaves (Fig. 3*B*). All the three types of leaves maintained their activity.

Prompt Chl *a* fluorescence: The newly emerged leaves were physiologically different from the older ones, and their stress responses might be different. The leaf reaction depends on its physiological conditions, including the age (Shen *et al.* 2007, Yordanov *et al.* 2008). Changes in plants' physiological state reflect in different course of Chl *a* fluorescence transitions during its characteristic phases O–K, O–J, J–I, and I–P. That is why we investigated responses to the infection in three types of leaves of different ages. Changes in the IC shape can be visualized by difference curves (DC) calculated as a difference in fluorescence values between stressed and control objects (Strasser 2004, Tsimilli-Michael and Strasser 2013a). The differences in the IC shapes during the characteristic phases are manifested as specific bands in DC: L band [between O and K (300 μs)], K band (O–J), H band (J–I), and G band

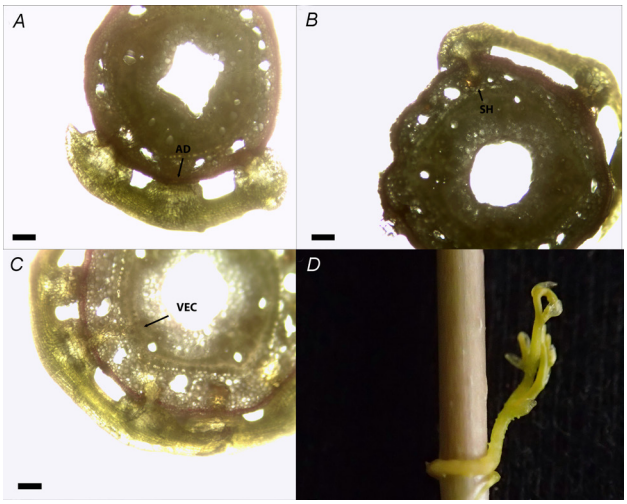

Fig. 2. Stages of *Cuscuta campestris* infection of *Ipomoea tricolor*. (*A*) Formation of adhesive disc (AD); (*B*) further penetration of searching hyphae (SH); (*C*) establishment of vascular elements connection (VEC); and (*D*) *C. campestris* growing on *I. tricolor* by the end of the experiment. Scale bar 100 μm.

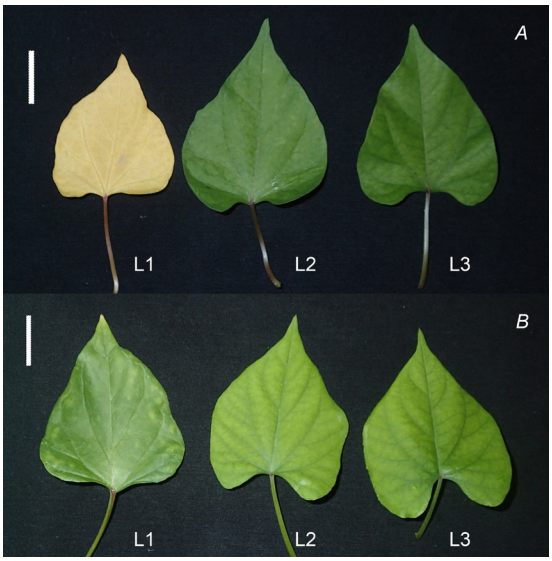

Fig. 3. *Ipomoea tricolor* leaves of different ages on the last, 35th day of the experiment (50th day of vegetation). Scale bar 2 cm. (*A*) Control plants. (*B*) Infected with *Cuscuta campestris* plants.

(I–P) (Strasser *et al.* 2004, Stirbet and Govindjee 2012). We carried out standard OJIP analysis of the IC of PF, and calculated DC to evaluate the influence of *C. campestris* infection on *I. tricolor* photosynthetic apparatus (PSA). The shape of the induction rise of Chl *a* fluorescence, measured on the leaves of control and infected *I. tricolor* plants, varied depending on both the age of the plant and the *C. campestris* infection.

We analyzed the changes induced by *C. campestris* infection in IC of PF in *I. tricolor* leaves in three steps: (*1*) Analysis of PF in leaves of different ages – L1, L2, and L3, from control *I. tricolor* plants. The effect of leaf senescence was revealed. (*2*) Analysis of PF in leaves of different ages – L1, L2, and L3, from *I. tricolor* plants infected with *C. campestris*. The effects of infection and senescence was revealed. (*3*) Analysis of the differences in PF in leaves of different ages – L1, L2, and L3, between control and infected *I. tricolor* plants. The effect of *C. campestris* infection was revealed. The dynamics of Chl *a* fluorescence changes in L1 leaves from control *I. tricolor* plants (averaged raw fluorescence transients), and the results from the first two steps of IC analysis are shown in Figs. 1S–7S (*supplement*).

O, J, I, and P characteristic steps of Chl *a* fluorescence IC were used for calculations of different JIP-test parameters and estimation of structural and functional changes in PSA. The calculated JIP-test parameters for the third step of the analysis for all the three types of leaves are shown below as spider plots (Fig. 7).

IC from infected and control *I. tricolor* plants: Both age-induced and infection-induced alterations were clearly visualized by differential curves of PF for control and infected *I. tricolor* plants (Figs. 1S–7S). However, what was the effect of the parasite *C. campestris* only? To evaluate its effect, we calculated the differences between the infected and the control plants. In this case, each DC value was calculated as a difference between the values of the relative variable fluorescence [$V_t = (F_t - F_O)/(F_M - F_O)$] recorded in the infected plants minus the respective values for the control plants [$\Delta V_t = V_{t(Cusc)} - V_{t(Contr)}$]. Thus, we were able to estimate *C. campestris* impact on the PSA in *I. tricolor* leaves without counting aging effects.

DC of the oldest leaves L1 from infected and control *I. tricolor* plants: The OJIP fluorescence rise reflects Q_A reduction, with Q_A poise depending on the poise of the intersystem electron carriers, which, in turn, depends also on the redox state of P700 (PSI reaction center). DC obtained for the oldest leaves – L1, showed that the *C. campestris* infection disrupted the balance throughout the whole system and simultaneously affected all phases of OJIP transients (Fig. 4*A*). The phases were not stable. The effects varied greatly over the vegetation period. The often-changing PSA characteristics reflected the host's struggle with the parasite. A depletion was observed after 35 d, when the highest positive differences were noticed.

L-band (50–300 μs): Changes in the differences in PF IC during the O–K time interval reflect the level of PSII grouping within the thylakoid membrane and the probability for redistribution of the excitation energy between them. The PSII antenna complexes are not fixed, they can move, they have changed during the plant growing and developing, and thus the efficiency of interaction between the antenna complexes has changed during the vegetation. Changes in L-band reveal if the PSII antenna complexes are energetically connected (grouped) or separated (ungrouped). The differences in the formed L band (~ 150 μs) may be positive or negative. Negative values mean greater grouping, and positive differences

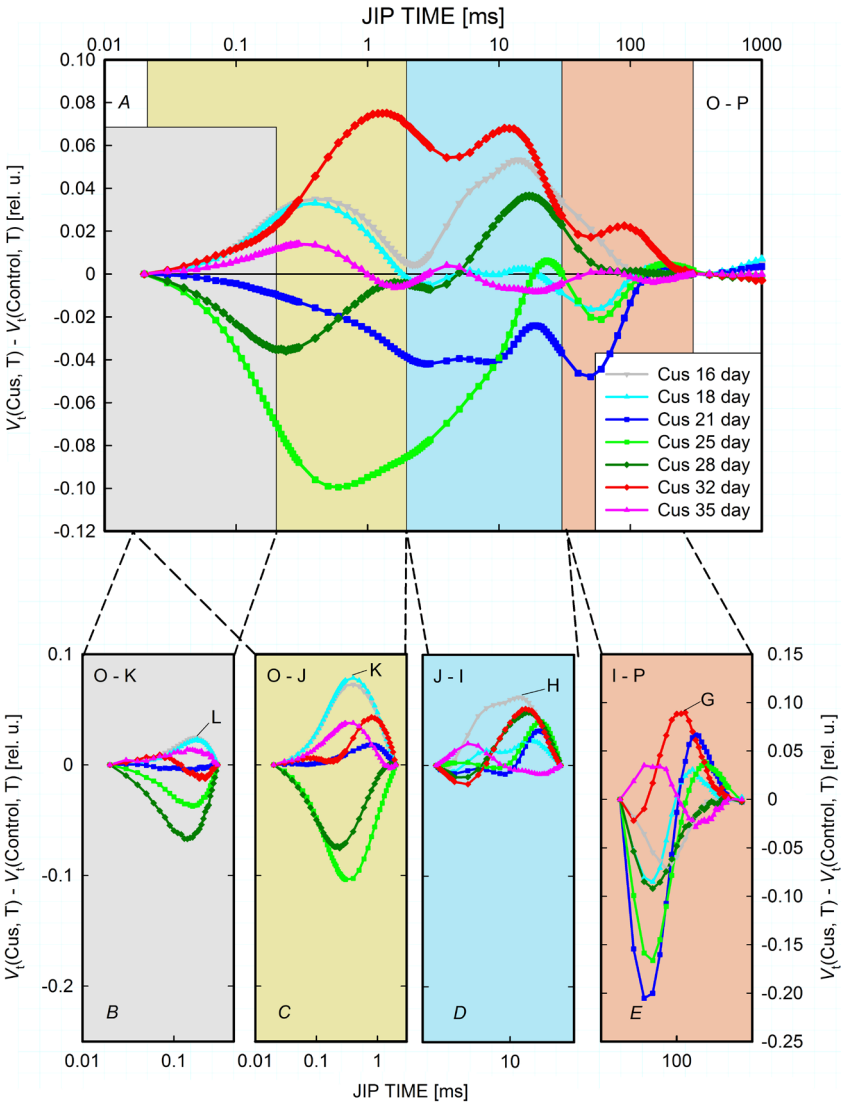

Fig. 4. Differential curves showing differences between the oldest L1 leaves from infected with *Cuscuta campestris* and control *Ipomoea tricolor* plants. Each DC value was calculated as a difference between the values of the relative variable fluorescence [$V_t = (F_t - F_O)/(F_M - F_O)$] recorded in first true leaves L1 of the infected plants minus the respective values for L1 of the control plants [$\Delta V_t = V_{t(Cusc)} - V_{t(Contr)}$]. The four characteristic bands are marked with different colors (*A*), and four additional panels (*B–E*) show details in each band. For panels *B–D* the values for the curves are related to the left scale of *y*-axes, for panel *E* to the right scale.

ungrouping of the antenna complexes (Tsimilli-Michael and Strasser 2013a).

Positive and negative L-bands (Fig. 4*B*) formed at the different terms of the investigation – in the infected plants the Chl synthesis was modified. Antenna complexes were activated on the days 25 and 28. At the last days of the investigation, slight exhausting and antennae inactivation were observed as a result of infection.

K-band (50 µs–2 ms): K-band reflects photochemical reduction of Q_A and partial reoxidation of Q_A^- by PQ (*via* Q_B). The K-band, formed in this phase at about 300 µs, provides information about the oxygen-evolving complex (OEC), particularly Mn-complex in PSII donor side (Strasser 1997, Yusuf *et al.* 2010, Stirbet *et al.* 2014). It characterizes the ratio of the electron transport rates between donor and acceptor side of PSII, and indicates how they function. The differences in K-band could be positive – due to slower electron transport from the donor side (because of OEC inactivation) and/or faster electron withdrawing from the acceptor side, or negative – because of faster electron transport from the donor side (electron transport acceleration) and/or slower withdrawing of electrons from the acceptor side (electron transport delay).

Both positive and negative differences in K-bands were formed in L1 (Fig. 4*C*). Some activation of the electron transport resulted in negative K-band values at 25 and 28 d. Afterwards, OEC inactivation took place in positive K-band forming.

H-band (2–30 ms): The shape of the DC from J- to I-steps reflects the dynamics of the reduction of the PQ pool between the two PS. Aging-induced alterations in the DCs were a result of changes in relative volumes of the PQ pool and the number of electrons required to fully reducing the PQ pool to level I. If the PQ pool capacity decreases, the rate of reduction will be higher and this will result in positive values of the transient band. Conversely, if the influenced factor (*C. campestris* infection in this case) increases the relative size of the PQ pool, there will be negative values for that band. H-band characterizes the PQ pool volume (number of active PQ molecules functioning

between the two PS), as well as the electron transfer to Q_A^- and the rate of electron withdraw from Q_A^-, so H-band represents the dynamics of reduction of PQ pool. Positive differences mean the PQ pool is relatively smaller, and negative – if the PQ pool is relatively bigger.

The positive values of the differences in H-bands in L1 leaves (Fig. 4*D*) demonstrated that *C. campestris* infection affected mainly the slow reducing part of PQ pool in the oldest leaves. PQ pool was relatively small in the infected plants, and bigger in the control ones.

G-band (30–300 ms): This interval reflects the reduction of the PSI end electron acceptors and the rate of this reduction determines the shape of G-band. With a larger end acceptors pool, the rising to the maximum will be slower, and this will be manifested in negative values of the transient band. If the pool of PSI end electron acceptors decreases, the transient will be faster, and a positive peak in the DCs will appear. This curve gives information about the PSI functioning and reoxidation of the PQ pool from PSI carriers.

G-band characterizes the PSI end electron acceptors condition, and the relative size of end PSI acceptors pool could be estimated. The differences in G-band will be positive when the acceptors pool is relatively smaller; and negative – if the pool is bigger. The amplitude of the differences (with maximum at about 150–200 ms) informs about electron transfer between the pool of reduced PQ and the pool of PS1 end acceptors.

There were two phases in G-band of the DC. Negative values of the differences between infected and control *I. tricolor* plants revealed an increase of the relative size of the PQ pool in the infected plants, and the positive values evinced an increase of the easily accessible molecules. On 32 d, the negative amplitude in DC was very small, and differences turned to positive values earlier. On the last day (35^{th}) the differences were with positive values until 100 ms, and negative ones during the second half of the G-band. A probable reason for this biphasic signal pattern might be a heterogeneity in electron acceptors ($NADP^+$) localization in relation to the acceptor side of PSI. By decreasing the relative part of the more accessible acceptors, their reduction will accelerate and this will lead to formation of positive amplitudes in DC, and *vice versa* – increasing of the accessible acceptors will slow down their reduction and negative amplitudes will be formed.

DC of the L2 leaves from infected and control *I. tricolor* plants: The differences in the fluorescence IC between younger leaves L2 in infected and control *I. tricolor* plants are shown on Fig. 5*A*. L2 leaves were measured from 16 to 35 d. A depletion in the leaves from infected plants was revealed.

There were not big differences between infected and control plants during O–K phase from 18 to 32 d – just tiny negative values of L-bands (Fig. 5*B*). L-band positive values on the first measurement (16 d) and at the end of the investigated period (35 d) reflected the first reaction of the youngest L2 leaves from the infected plants, and some exhausting at the end of the experiment.

K-band positive values on 16 and 18 d reflected OEC inactivation in L2 leaves of infected plants. Then some adaptation took place and K-band negative values from 21 to 32 d indicated electron transport activation (Fig. 5*C*). An exhaustion at the end of the period (35 d) was revealed by positive K-band.

The positive differences in H-band (except 21 d) meant relatively small PQ pool, and suppression of its reduction as a result of *C. campestris* infection (Fig. 5*D*). The most interesting were *C. campestris* effects on G-band (Fig. 5*E*). The positive values of the differences were probably a result of decreasing the pool of PSI end electron acceptors in infected plants. At the 35 d, the relative size of $NADP^+$ pool increased (a strong negative peak), probably due to some retarding effect of *C. campestris* on aging processes.

DC from the youngest leaves L3 from infected and control *I. tricolor* plants: The differences in IC from youngest leaves L3 of infected and control *I. tricolor* plants are shown in Fig. 6. L3 appeared and developed entirely in the *C. campestris* presence. The first measurement for these leaves was at 18 d of the investigation, when the biggest positive differences were observed (Fig. 6*A*). Afterward the differences decreased gradually until 28 d, and slightly increased in the latest periods. A well-pronounced relative ungrouping of antenna complexes in infected plants was visible in L-band on 18 d (Fig. 6*B*), after that their grouping was almost the same as in control plants. The strong positive K-band at the same, 18 d, indicated strong L3 reaction to the infection, with OEC inactivation and slower electron transfer to PSI donor side, and probably faster electron uptake to the acceptor side (Fig. 6*C*). The PQ pool was relatively small in the infected plants, and all the differences were positive (Fig. 6*D*). The relative size of $NADP^+$ pool was bigger in the L3 leaves from the infected plants in comparison with the control ones (Fig. 6*E*).

The youngest L3 leaves showed strong response to *C. campestris* infection on the first measurement, 18 d, when they just appeared. Later, they adapted to the parasite, and all of the PF parameters were close to the control ones during the investigated period.

Dynamics of the differences in the IC during the whole investigated period revealed that the parasite effects on host leaves were different for each of the four phases, and strongly depended on the leaves age. Detailed analysis of the differences between the infected and control plants during the four characteristic phases is given in supplementary information (Fig. 8S, *supplement*).

JIP-test parameters provide better visualization of effects of *C. campestris* infection on *I. tricolor* leaves of different ages (L1, L2 and L3). As presented in Fig. 7, 17 JIP parameters were calculated from the induction curves of the prompt Chl *a* fluorescence as a ratio of the parameter value for infected plants to the value of the same parameter, the same day, for control plants. Thus, obtained ratios for a certain parameter were normalized to the maximal value

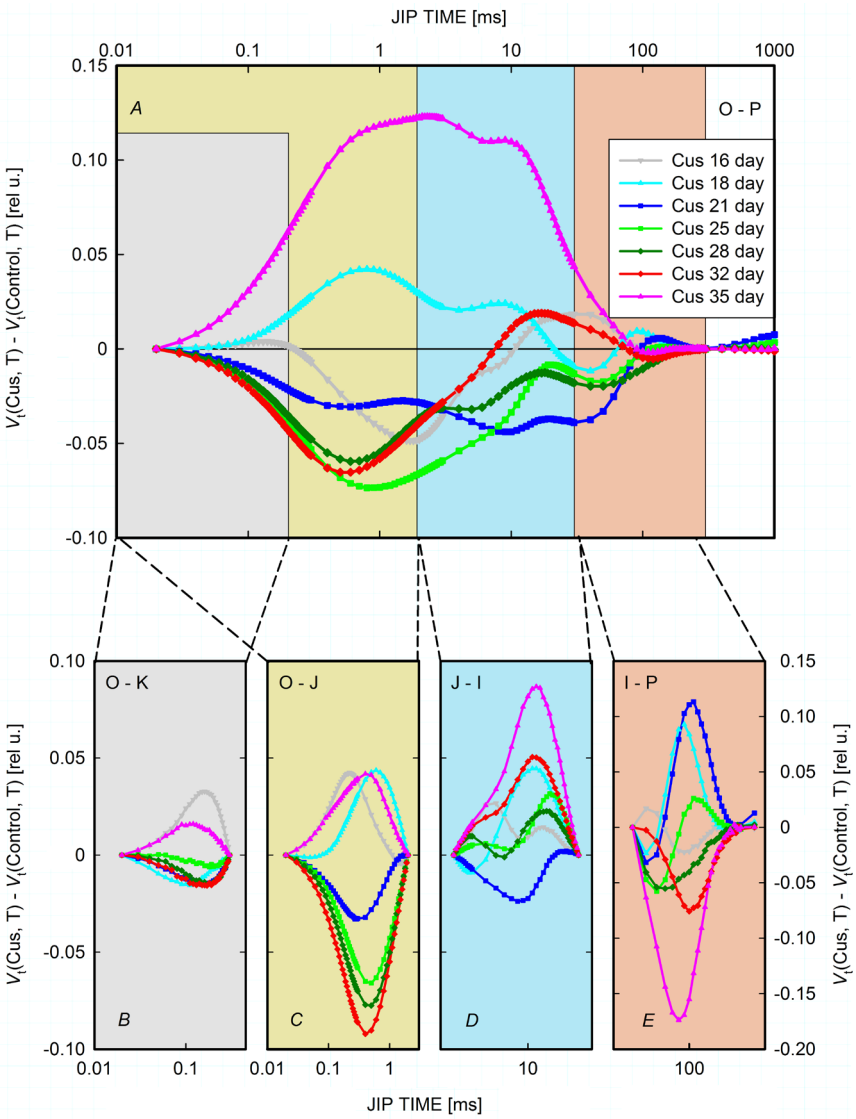

Fig. 5. Differential curves showing differences between younger leaves L2 from infected with *Cuscuta campestris* and control *Ipomoea tricolor* plants. Each DC value was calculated as a difference between the values of the relative variable fluorescence $[V_t = (F_t - F_O)/(F_M - F_O)]$ recorded in the second true leaves L2 of the infected plants minus the respective values for the L2 of control plants $[\Delta V_t = V_{t(Cusc)} - V_{t(Contr)}]$. The four characteristic bands are marked with different colors (*A*), and four additional panels (*B–E*) show details in each band. For panels *B–D* the values for the curves are related to the left scale of *y*-axes, for panel *E* to the right scale.

of that parameter.

For all the three types of leaves, the parameters performance index of PSII (PI_{ABS}) and performance index of both photosystems (PI_{total}) were very sensitive to the *C. campestris* infection. PI_{ABS} describes PSII condition and how it works. In the oldest L1 and L2, some inactivation was observed – the PI_{ABS} values decreased in comparison to the 16th d. L3 responses to the infection were opposite, *i.e.*, increased values compared to the first measurement at 18 d, which means PSII activation in the parasite presence. PI_{total} is a parameter giving us information about the functioning of both PSI and PSII. It showed some activation of PSI due to the infection – on 28 and 32 d for L1, on 21–28 d for L2, and on 21 and 25 d for L3. Another parameter, the number of Q_A redox turnovers until maximal fluorescence (F_M) is reached (N), was significantly affected in L3 by the parasite *C. campestris*, *i.e.*, the number of electrons needed for full reduction of all the carriers after Q_A until reaching F_M – the electron flow decreases due to the activation of the reaction centers (γ_{RC} increased). The most stable was the parameter φ_{P0}, the quantum yield of the primary photochemical reactions of PSII; it almost did not change under the infection.

Influence of dodder parasitism on the photosynthetic apparatus and aging of leaves: The plant functions as a unitary, complex system with constant interaction between its different organs. Newly developing leaves need nutrients and energy, which they obtain from earlier appeared, older leaves. First, embryonic leaves, exist and work until the true leaves develop, then senescence begins, and finally they wither. Programmed cell death by apoptosis accompanies aging processes, but senescence depends not only on the age of the leaf, it is more related to whether the plant needs that leaf or if the need is already eliminated (Lim *et al.* 2007). In our experiment, the aging of the leaves was delayed because the plant needed them to compensate for the effect of the parasite. Delayed leaf senescence in infected plants, resulting in stimulation of canopy photosynthesis, was reported by Press *et al.*

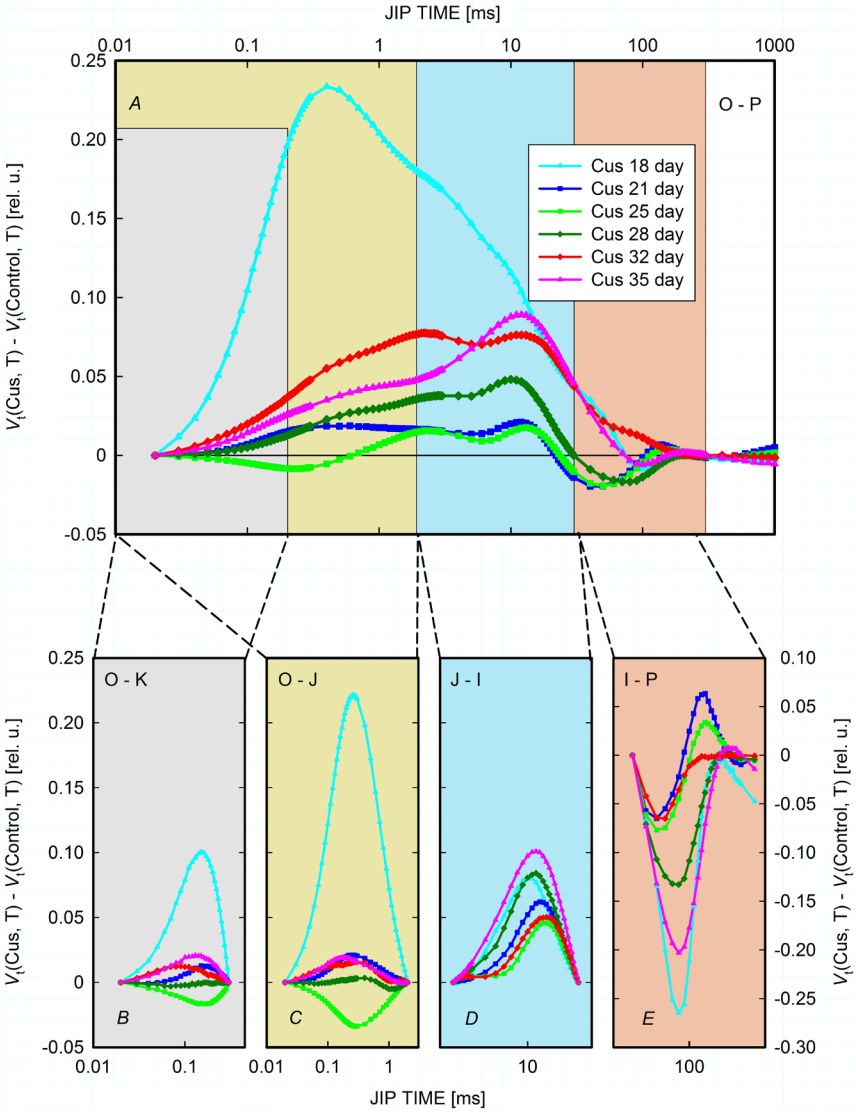

Fig. 6. Differential curves showing differences between the youngest leaves L3 from infected with *Cuscuta campestris* and control *Ipomoea tricolor* plants. Each DC value was calculated as a difference between the values of the relative variable fluorescence [$V_t = (F_t - F_O)/(F_M - F_O)$] recorded in third true leaves L3 of the infected plants minus the respective values for the L3 of control plants [$\Delta V_t = V_{t(Cusc)} - V_{t(Contr)}$]. The four characteristic bands are marked with different colors (*A*), and four additional panels (*B–E*) show details in each band. For panels *B–D* the values for the curves are related to the left scale of *y*-axes, for panel *E* to the right scale.

(1999). In our previous studies, we have demonstrated that decapitation (removing the apical bud) of bean plants not only delayed the senescence in primary (embryonic) leaves but induced rejuvenation in the leaf cells revealed by prompt and delayed Chl fluorescence analysis (Yordanov *et al.* 2008).

PSA is a very sensitive structure, and its functioning changes under even slight stress. JIP-test allows us to reveal small alterations in PSA condition and functioning (Kalaji *et al.* 2014c, 2016, 2017) The JIP-analysis of the effects of parasite *C. campestris* on *I. tricolor* plants revealed differences in sensitivity of different processes in PSA.

C. campestris effect on the antenna complexes grouping in the investigated three types *I. tricolor* leaves of different ages was relatively small, with a tendency (more noticeable in the youngest leaves L3) for some ungrouping in the first days after the infection.

There was some similarity in dynamics of the electron transfer between donor and acceptor side of PSII (K-band) in leaves L1 and L2. The first plant response to the infection was an inactivation of OEC, slower electron transport from donor side, and retarded electron withdrawing from acceptor side observed in infected plants in first days. Infected *I. tricolor* plants were fighting the parasite by activating the electron transport in PSII in late periods (negative K-band). Small positive K-band showed little OEC activation and slower electron transfer at the end of the investigation period, *i.e.*, some adaptation of the host plant.

L3 leaf responses were different – after the first OEC inactivation, slower electron transfer in PSII, an adaptation to the parasite occurred and the K-peaks values of infected plants were equal to the control ones.

Cuscuta campestris infection resulted in a slight but lasting decrease in the PQ pool size – all the differences in H-band between infected and control plants had positive values, except for day 21 in L2. The most interesting was the dynamics of the accessible end electron acceptors of PSI manifested by differences in G-band. The *C. campestris* effect on I–P phase was quite different in the three types of *I. tricolor* leaves; the biggest differences

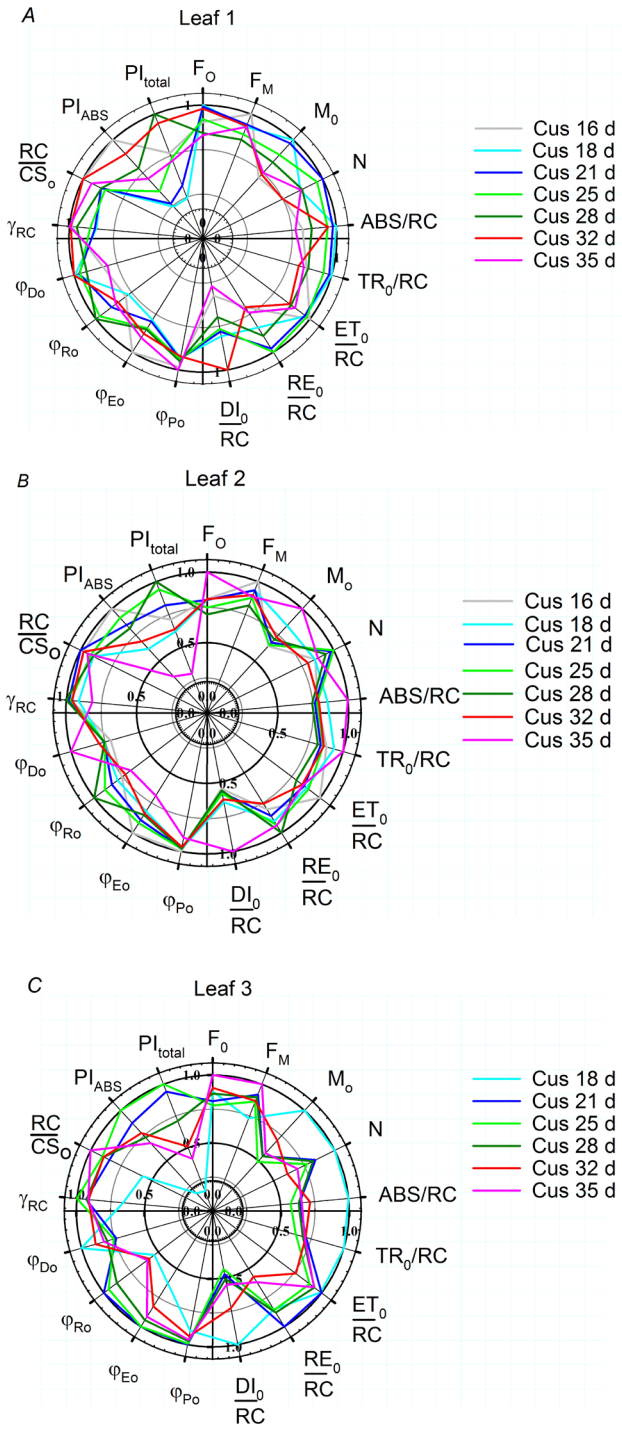

Fig. 7. JIP-test parameters in leaves of different ages (L1, L2, and L3) calculated from the induction curves of the prompt Chl *a* fluorescence as a ratio of the parameter value for *Ipomoea tricolor* infected with *Cuscuta campestris* plants to the value of the same parameter, the same day, for control plants. Thus obtained ratios for a certain parameter were normalized to the maximal value for that parameter.

between infected and control plants were observed during that transition. The oldest leaves L1 responded to the infection by increasing the size of PSI end acceptors until 28 d; the decrease was found after 32 and 35 d. Completely opposite reactions were observed in the younger leaves L2 – a reduced size of accessible PSI end electron acceptors until 25 d, and the increased size during the latest periods. In the youngest leaves L3, the number of accessible PSI end acceptors was bigger than that in control leaves during the whole period with maximal difference on day 18; an exception occurred after 21 d, when a small positive difference was observed.

The oldest leaves L1, which were well developed before infection, responded to the parasite until day 28, then some adaptation occurred, and the values of the four characteristic bands were close to the control ones.

Electron transport reactions (O–J and I–P transitions) were the most sensitive to *C. campestris* infection in L2 leaves. Those leaves did not achieve adaptation to the parasite.

The youngest L3 leaves appeared after the infection, and they were completely developing under *C. campestris* influence. They reacted strongly at the first day of the measurement – 18th d of the experiment, after that, they achieved some adaptation, and, except G-band, the characteristic phase values were close to the control ones. They did not reach leaf senescence during the experiment.

Conclusion: The fact that different areas of the IC were affected means that the *C. campestris* infection influenced the entire electron transport chain in all of the *I. tricolor* leaves. PSA reactions to the *C. campestris* infection depended on the leaf age but for all the three types of leaves, I–P transient was the most sensitive to the infection. Our results are in agreement with the results of Shen *et al*. (2007) who found that changes in photosynthetic reactions in leaves of *Mikania micrantha*, infected with *C. campestris*, depended on the leaf age. The presence of the parasite *C. reflexa* induced a sink-dependent stimulation of net photosynthesis in host and caused a delay in leaf senescence in *Ricinus communis* (Jeschke and Hilpert 1997) and in *Coleus blumei* (Jeschke *et al.* 1997). Further studies on the influence of the parasite *C. campestris* on its hosts are needed to reveal mechanisms of parasite-host interaction and to develop more effective methods for control and prevention of crop infestation with *C. campestris*. JIP-test analysis of Chl *a* fluorescence is a very perspective method for assessment of those interaction mechanisms.

References

Chen S., Strasser R.J., Qiang S.: *In vivo* assessment of effect of phytotoxin tenuazonic acid on PSII reaction centers. – Plant Physiol. Bioch. **84**: 10-21, 2014.

Dinelli G., Bonetti A., Tibiletti E.: Photosynthetic and accessory pigments in *Cuscuta campestris* Yuncker and some host species. – Weed Res. **33**: 253-260, 1993.

Jeschke W.D., Baig A., Hilpert A.: Sink-stimulated photosynthesis, increased transpiration and increased demand-dependent stimulation of nitrate uptake: Nitrogen and carbon relations in the parasitic association *Cuscuta reflexa-Coleus blumei*. – J. Exp. Bot. **48**: 915-925, 1997.

Jeschke W.D., Hilpert A.: Sink-stimulated photosynthesis and

sink-dependent increase in nitrate uptake: nitrogen and carbon relations of the parasitic association *Cuscuta reflexa-Ricinus communis*. – Plant Cell Environ. **20**: 47-56, 1997.

Kalaji H.M., Jajoo A., Oukarroum A. *et al.*: The use of chlorophyll fluorescence kinetics analysis to study the performance of photosynthetic machinery in plants. – In: Ahmad P., Rasool S. (ed.): Emerging Technologies and Management of Crop Stress Tolerance. Pp. 347-384. Elsevier, San Diego 2014a.

Kalaji H.M., Jajoo A., Oukarroum A. *et al.*: Chlorophyll *a* fluorescence as a tool to monitor physiological status of plants under abiotic stress conditions. – Acta Physiol. Plant. **38**: 102, 2016.

Kalaji H.M., Oukarroum A., Alexandrov V. *et al.*: Identification of nutrient deficiency in maize and tomato plants by *in vivo* chlorophyll *a* fluorescence measurements. – Plant Physiol. Bioch. **81**: 16-25, 2014b.

Kalaji H.M., Schansker G., Brestič M. *et al.*: Frequently asked questions about chlorophyll fluorescence, the sequel. – Photosynth. Res. **132**: 13-66, 2017.

Kalaji H.M., Schansker G., Ladle R.J. *et al.*: Frequently asked questions about *in vivo* chlorophyll fluorescence: practical issues. – Photosynth. Res. **122**: 121-158, 2014c.

Kautsky H., Hirsch A.: Neue Versuche zur Kohlensäureassimilation. – Naturwissenschaften **19**: 964-964, 1931.

Le Q.V., Tennakoon K.U., Metali F. *et al.*: Impact of *Cuscuta australis* infection on the photosynthesis of the invasive host, *Mikania micrantha*, under drought condition. – Weed Biol. Manag. **15**: 138-146, 2015.

Lim P.O., Kim H.J., Nam H.G.: Leaf senescence. – Annu. Rev. Plant Biol. **58**: 115-136, 2007.

McNeal J.R., Kuehl J.V., Boore J.L., de Pamphilis C.W.: Complete plastid genome sequences suggest strong selection for retention of photosynthetic genes in the parasitic plant genus *Cuscuta*. – BMC Plant Biol. **7**: 57, 2007.

Parker C.: Parasitic weeds: a world challenge. – Weed Sci. **60**: 269-276, 2012.

Press M.C., Graves J., Stewart G.: Physiology of the interaction of angiosperm parasites and their higher plant hosts. – Plant Cell Environ. **13**: 91-104, 1990.

Press M.C., Scholes J.D., Watling J.R.: Parasitic plants: Physiological and ecological interactions with their host. – In: Press M.C., Scholes J.D., Barker M.G. (ed.): Physiological Plant Ecology: 39th Symposium of the British Ecological Society. Pp. 175-197. Blackwell Science, Oxford 1999.

Revill M.J., Stanley S., Hibberd J.M.: Plastid genome structure and loss of photosynthetic ability in the parasitic genus *Cuscuta*. – J. Exp. Bot. **56**: 2477-2486, 2005.

Sarić-Krsmanović M., Božić D., Radivojević L. *et al.*: Impact of field dodder (*Cuscuta campestris* Yunk.) on chlorophyll fluorescence and chlorophyll content of alfalfa and sugar beet plants. – Russ. J. Plant Physl+ **65**: 726-731, 2018.

Shen H., Hong L., Ye W. *et al.*: The influence of the holoparasitic plant *Cuscuta campestris* on the growth and photosynthesis of its host *Mikania micrantha*. – J. Exp. Bot. **58**: 2929-2937, 2007.

Shen H., Ye W., Hong L. *et al.*: Influence of the obligate parasite *Cuscuta campestris* on growth and biomass allocation of its host *Mikania micrantha*. – J. Exp. Bot. **56**: 1277-1284, 2005.

Singh A., Singh M.: Incompatibility of *Cuscuta* haustoria with the resistant hosts – *Ipomoea batatas* L. and *Lycopersicon esculentum* Mill. – J. Plant Physiol. **150**: 592-596, 1997.

Stirbet A., Govindjee: On the relation between the Kautsky effect (chlorophyll *a* fluorescence induction) and Photosystem II: basics and applications of the OJIP fluorescence transient. – J. Photoch. Photobio. B **104**: 236-257, 2011.

Stirbet A., Govindjee: Chlorophyll *a* fluorescence induction: a personal perspective of the thermal phase, the J-I-P rise. – Photosynth. Res. **113**: 15-61, 2012.

Stirbet A., Riznichenko G.Y., Rubin A.: Modeling chlorophyll *a* fluorescence transient: relation to photosynthesis. – Biochemistry-Moscow+ **79**: 291-323, 2014.

Strasser B.: Donor side capacity of Photosystem II probed by chlorophyll *a* fluorescence transients. – Photosynth. Res. **52**: 147-155, 1997.

Strasser R.J., Srivastava A., Tsimilli-Michael M.: The fluorescence transient as a tool to characterize and screen photosynthetic samples. – In: Yunus M., Pathre U., Mohanty P. (ed.): Probing Photosynthesis: Mechanisms, Regulation and Adaptation. Pp. 445-483. Taylor & Francis, London 2000.

Strasser R.J., Tsimilli-Michael M., Qiang S., Goltsev V.: Simultaneous *in vivo* recording of prompt and delayed fluorescence and 820-nm reflection changes during drying and after rehydration of the resurrection plant *Haberlea rhodopensis*. – BBA-Bioenergetics **1797**: 1313-1326, 2010.

Strasser R.J., Tsimilli-Michael M., Srivastava A.: Analysis of the chlorophyll *a* fluorescence transient. – In: Papageorgiou G.C., Govindjee (ed.): Chlorophyll *a* Fluorescence: A Signature of Photosynthesis. Advances in Photosynthesis and Respiration. Pp. 321-362. Springer, Dordrecht 2004.

Tsimilli-Michael M., Strasser R.J.: *In vivo* assessment of stress impact on plants' vitality: applications in detecting and evaluating the beneficial role of mycorrhization on host plants. – In: Varma A. (ed.): Mycorrhiza. State of the Art, Genetics and Molecular Biology, Eco-Function, Biotechnology, Eco-Physiology, Structure and Systematics. 3rd edition. Pp. 679-703. Springer, Berlin-Heidelberg 2008.

Tsimilli-Michael M., Strasser R.J.: The energy flux theory 35 years later: formulations and applications. – Photosynth. Res. **117**: 289-320, 2013a.

Tsimilli-Michael M., Strasser R.J.: Biophysical phenomics: Evaluation of the impact of mycorrhization with *Piriformospora indica*. – In: Varma A., Kost G., Oelmüller R. (ed.): *Piriformospora indica*. Sebasinales and their Biotechnological Applications. Pp. 173-190. Springer-Verlag, Berlin-Heidelberg 2013b.

Yordanov I., Goltsev V., Stefanov D. *et al.*: Preservation of photosynthetic electron transport from senescence-induced inactivation in primary leaves after decapitation and defoliation of bean plants. – J. Plant Physiol. **165**: 1954-1963, 2008.

Yoshida S., Cui S., Ichihashi Y., Shirasu K.: The haustorium, a specialized invasive organ in parasitic plants. – Annu. Rev. Plant Biol. **67**: 643-667, 2016.

Yu H., Liu J., He W.-M. *et al.*: *Cuscuta australis* restrains three exotic invasive plants and benefits native species. – Biol. Invasions **13**: 747-756, 2011.

Yusuf M.A., Kumar D., Rajwanshi R. *et al.*: Overexpression of γ-tocopherol methyl transferase gene in transgenic *Brassica juncea* plants alleviates abiotic stress: Physiological and chlorophyll *a* fluorescence measurements. – BBA-Bioenergetics **1791**: 1428-1438, 2010.

Zhang L., Liu J.: Effects of heat stress on photosynthetic electron transport in a marine cyanobacterium *Arthrospira* sp. – J. Appl. Phycol. **28**: 757-763, 2016.

Appendix. Definition of selected OJIP parameters according to Strasser *et al.* (2004) and Stirbet and Govindjee (2011).

Parameter	Definition
F_O	Minimal fluorescence, when all PSII reaction centers (RCs) are open, fluorescence intensity at 20 μs
$F_M = F_P$	Maximal fluorescence recorded under saturating illumination at the peak P of OJIP, when all PSII RCs are closed
F_J (2 ms)	Fluorescence level at 2 ms, the J-step of OJIP
F_I (30 ms)	Fluorescence level at 30 ms, the I-step of OJIP
F_V	Maximal variable fluorescence, $F_V = F_M - F_O$
F_V/F_M	The maximum quantum yield of primary photochemical reactions in PSII RC
V_t	Relative variable fluorescence at time t: $V_t = (F_t - F_0)/(F_M - F_O)$
V_L	Relative fluorescence value at L-step [0.15 ms]
V_K	Relative fluorescence value at K-step [0.3 ms]
M_0	Approximated initial slope of the fluorescence transient, $M_0 = 4\ (F_{0.3ms} - F_O)/(F_M - F_O)$
N	Number indicating how many times Q_A is reduced until fluorescence reaches its maximal value F_M (number of Q_A redox turnovers until F_M is reached)
ABS	Absorbed energy flux (exited PSII antennae Chl *a* molecules)
TR_0	Trapped energy, *i.e.*, energy utilized for reduction of pheophytin and primary quinone acceptor Q_A
ET_0	Electron transport from Q_A^- to the next electron acceptors between the two photosystems
RE_0	Energy/electron flux for reduction of end acceptors in acceptor side of PSI – NADP and ferredoxin
φ_{Eo} (ET_0/ABS)	Efficiency/probability for the electron in PSII to move further than Q_A^- – quantum yield for electron transport, $\varphi_{Eo} = ET_0/ABS = \varphi_{Po} \times \psi_0 = (1 - F_O/F_M)\ \psi_0$
ψ_0 (ET_0/TR_0)	Efficiency of the trapped exciton to transfer an electron from Q_A^- to the next electron acceptors over the electron transport chain between the two photosystems, $\psi_0 = ET_0/TR_0 = 1 - V_J$
ρ_0 (RE_0/TR_0)	Efficiency of the trapped exciton to transfer an electron over the electron transport chain from Q_A^- to the end electron acceptors of PSI, $\rho_0 = RE_0/TR_0 = \psi_0 \times \delta_0$
ABS/RC	Absorbed energy flux in antenna chlorophylls per PSII reaction center (a measure of PSII apparent antenna size)
TR_0/RC	Trapped energy flux per RC, $TR_0/RC = M_0\ (1/V_J)$
ET_0/RC	Electron transport flux further than Q_A^- per PSII reaction center
DI_0/RC	Dissipated energy flux per PSII reaction center at t = 0
RE_0/RC	Electron flux reducing end electron acceptors at the PSI acceptor side, per PSII reaction center
DI_0/RC	Heat dissipation of excitation energy by PSII reaction center
ET_0/RC	Electron transport flux further than Q_A^- per PSII reaction center
φ_{Po} (TR_0/ABS)	Maximum quantum yield of primary photochemical reactions in PSII RC, $\varphi_{Po} = TR_0/ABS = 1 - F_O/F_M$
δ_{R0} (RE_0/ET_0)	Efficiency/probability for an electron to be transferred from reduced carriers between the two photosystems to the end acceptors of PSI, $\delta_0 = RE_0/ET_0 = (1 - V_I)/(1 - V_J)$
φ_{Ro} (RE_0/ABS)	Quantum yield of the electron transport from Q_A^- to the end electron acceptors of PSI, $RE_0/ABS = \varphi_{Ro} = \varphi_{Po} \times \psi_0 \times \delta_0$
φ_{Do}	Expresses the probability for the energy of absorbed photon to dissipate as heat, the quantum yield of energy dissipation at time zero, $\varphi_{Do} = 1 - \varphi_{Po} = F_O/F_M$
γ_{RC}	Probability for given chlorophyll *a* molecule in PSII to be a reaction center
RC/CS_0	Density of active PSII reaction centers (RC) per cross section , $RC/CS_0 = \varphi_{Po} \times (V_J/M_0) \times (ABS/CS_0)$
PI_{ABS}	Performance index (potential) for conservation the energy absorbed by PSII RC until the reduction of intersystem electron acceptors
PI_{total}	Performance index (potential) for conservation the energy absorbed by PSII until the reduction of PSI end electron acceptors